Stem Cell Reports
Article

ISSCR

OPEN ACCESS

Neural Crest Cell Implantation Restores Enteric Nervous System Function and Alters the Gastrointestinal Transcriptome in Human Tissue-Engineered Small Intestine

Christopher R. Schlieve,[1,2] Kathryn L. Fowler,[1] Matthew Thornton,[3] Sha Huang,[4,5,6] Ibrahim Hajjali,[1] Xiaogang Hou,[1] Brendan Grubbs,[3] Jason R. Spence,[4,5,6] and Tracy C. Grikscheit[1,2,*]

[1]Developmental Biology and Regenerative Medicine Program, The Saban Research Institute at Children's Hospital Los Angeles, 4650 W. Sunset Boulevard, MS#100, Los Angeles, CA 90027, USA
[2]Department of Surgery, Division of Pediatric Surgery, Children's Hospital Los Angeles, Los Angeles, CA, 90027, USA
[3]Department of Obstetrics and Gynecology, University of Southern California, Los Angeles, CA, 90033, USA
[4]Department of Internal Medicine, Division of Gastroenterology, University of Michigan Medical School, Ann Arbor, MI, 48109, USA
[5]Center for Organogenesis, University of Michigan Medical School, Ann Arbor, MI, 48109, USA
[6]Department of Cell and Developmental Biology, University of Michigan Medical School, Ann Arbor, MI, 48109, USA
*Correspondence: tgrikscheit@chla.usc.edu
http://dx.doi.org/10.1016/j.stemcr.2017.07.017

SUMMARY

Acquired or congenital disruption in enteric nervous system (ENS) development or function can lead to significant mechanical dysmotility. ENS restoration through cellular transplantation may provide a cure for enteric neuropathies. We have previously generated human pluripotent stem cell (hPSC)-derived tissue-engineered small intestine (TESI) from human intestinal organoids (HIOs). However, HIO-TESI fails to develop an ENS. The purpose of our study is to restore ENS components derived exclusively from hPSCs in HIO-TESI. hPSC-derived enteric neural crest cell (ENCC) supplementation of HIO-TESI establishes submucosal and myenteric ganglia, repopulates various subclasses of neurons, and restores neuroepithelial connections and neuron-dependent contractility and relaxation in ENCC-HIO-TESI. RNA sequencing identified differentially expressed genes involved in neurogenesis, gliogenesis, gastrointestinal tract development, and differentiated epithelial cell types when ENS elements are restored during *in vivo* development of HIO-TESI. Our findings validate an effective approach to restoring hPSC-derived ENS components in HIO-TESI and may implicate their potential for the treatment of enteric neuropathies.

INTRODUCTION

Enteric nervous system (ENS) development and function are governed by a broad array of regulatory molecules that are only partially known. Disruption of signaling pathways from congenital or acquired defects results in varying degrees of pathology (Lake and Heuckeroth, 2013). Among congenital enteric neuropathies, Hirschsprung's disease (HD) is the most common and is reported to arise from impaired migration of enteric neural crest cells (ENCCs) within the gut during fetal development, leading to functional obstruction from an inability to relax intestinal smooth muscle (Furness, 2012). Surgical resection of the distal aganglionic segment of intestine in HD decreases mortality, but does not result in complete resolution of symptoms (Laughlin et al., 2012; Sulkowski et al., 2014). The restoration of ENS components through cellular transplantation is a current goal for the treatment of gastrointestinal motility disorders (Burns et al., 2016).

ENS progenitor cells harvested from native intestine can differentiate into enteric neurons and functionally integrate into the gastrointestinal tract of mice (Cooper et al., 2016; Hetz et al., 2014; Hotta et al., 2016; Lindley et al., 2008). However, gastrointestinal-derived ENS progenitors have a limited capacity for self-renewal, reducing their ability to expand to sufficient numbers that may be required for therapeutic interventions (Bondurand et al., 2003; Finkbeiner et al., 2015; Kruger et al., 2002). In addition, they often contain a significant proportion of non-neural crest cell types, which may interfere with their ability to engraft, differentiate, and migrate in a reproducible manner (Binder et al., 2015). Our laboratory has previously demonstrated restoration of ENS neurons and glia in mouse and human tissue-engineered colon from patients with HD with supplementation of murine enteric neurospheres (Wieck et al., 2016). Although this supports the possibility that neurosphere implantation could provide a feasible means for restoring an ENS in aganglionic intestine, the likely need for repeat biopsies to harvest sufficient numbers of enteric neural progenitors may limit this approach in clinical practice (Friedt and Welsch, 2013; Metzger et al., 2009b).

In previous work, we have generated tissue-engineered small intestine (TESI) derived from human intestinal organoids (HIOs) (Spence et al., 2011; Watson et al., 2014) that closely resembles native human intestine (Finkbeiner et al., 2015). Although HIO-TESI contains mesenchymal cell types that are crucial for intestinal function, including fibroblasts, smooth muscle myocytes, and subepithelial myofibroblasts, an ENS does not develop. Recently, Workman

et al. demonstrated an approach to restore an ENS in HIOs by supplementation *in vitro* with ENCCs. However, the ENS formed by this approach was underdeveloped, as demonstrated by the presence of immature ganglia, the absence of neuroepithelial connections, and the loss of neuronal cell diversity after *in vivo* implantation (Workman et al., 2017). Therefore, alternative approaches must be explored in order to establish mature ENS function in aganglionic tissues.

In this study, we aim to (1) generate TESI derived exclusively from human pluripotent stem cells (hPSCs) and restore elements of ENS function, which could represent a future therapeutic intervention for patients suffering from short bowel syndrome or intestinal failure, (2) evaluate transcriptome changes that occur in HIO-TESI after *in vivo* development with and without ENS cell types, and (3) demonstrate a proof-of-concept approach for ENCC implantation into an intestinal aganglionosis model for the potential treatment of enteric neuropathies. We demonstrate successful establishment of components of the ENS in HIO-TESI derived solely from hPSCs. Furthermore, *in vivo* co-implantation promotes the formation of neuroepithelial connections important for intraluminal signaling, which fail to form when ENCCs are co-cultured *in vitro* with HIOs prior to *in vivo* implantation (Workman et al., 2017). Transcriptome-wide RNA sequencing (RNA-seq) analysis further established differences in the expression profile of genes responsible for gastrointestinal tract development, intestinal stem cell homeostasis, and differentiation of epithelial subpopulations. Our results suggest that early *in vivo* co-implantation of hPSC-derived ENCCs and HIOs to produce ENCC-HIO-TESI is an advantageous approach for establishing mature ENS function in tissue-engineered organs and may eventually restore function in patients with enteric neuropathies.

RESULTS

hPSC-Derived ENCCs Establish Neurons and Glia within the Submucosal and Myenteric Regions of HIO-Derived TESI

We have previously reported the successful derivation of human ENCCs that could differentiate into enteric neurons and glia, migrate to colonize the mouse intestine *in vitro* and *in vivo*, and engraft and rescue disease-related mortality in an HD mouse model (Fattahi et al., 2016). To establish an ENS in developing HIO-TESI, we selected the approach of implanting ENCC neurospheres after human embryonic stem cell (hESC)/human induced pluripotent stem cell (hiPSC)-directed differentiation (Figure 1A). In brief, H9 hESCs were directed into HIOs and expanded in culture for 28 to 35 days, as described previously (Finkbeiner et al., 2015). Concurrently, ENCCs were derived from unmodified hPSCs exposed to small-molecule inhibitors, as reported previously, until day 11 (Fattahi et al., 2016). Unsorted ENCCs were plated at day 11 into ultra-low attachment plates and cultured for an additional 4 days to form neurospheres prior to co-implantation with HIOs (Figure 1A). To confirm their ability to give rise to ENS cell types, ENCCs were separately cultured *in vitro* for an additional 40 days. Immunostaining revealed that ENCCs were of an enteric lineage (TRKC/RET/EDNRB-positive), and differentiated into excitatory neurons (CHAT-positive), inhibitory neurons (nNOS- and GABA-positive), and glia (SOX10/S100β-positive or SOX10/GFAP-positive) (Figure S2). To generate ENCC-HIO-TESI, unsorted day 15 ENCC neurospheres were transplanted with day 28–35 HIOs on scaffolds and sutured into the greater omentum of irradiated non-obese diabetic/severe combined immunodeficiency (NOD/SCID) mice as described previously (Barthel et al., 2012a, 2012b; Finkbeiner et al., 2015; Grant et al., 2015; Grikscheit et al., 2003), and allowed to mature *in vivo* for 3 months (Figure 1A). After 3 months, ENCC-HIO-TESI grew into cystic structures with prominent lumens (Figures 1B and 1C). H&E evaluation of ENCC-HIO-TESI cross-sections revealed mature intestinal development with villi and crypt-like structures, underlying smooth muscle myocytes and myofibroblasts, and the presence of submucosal and myenteric ganglia (Figures 1E and 1G). Ganglia were absent in all HIO-TESI that were not supplemented with ENCCs (Figures 1D and 1F).

After identifying ganglia by H&E, we further examined ENCC-HIO-TESI to classify specific cell types of the ENS. TUJ1-positive neurons were found in the submucosa and muscular layers (Figure 2A). GFAP-positive glia did not associate with submucosal ganglia or myenteric ganglia (Figure 2A). However, enteric S100β-positive glia were detected throughout the submucosa and within submucosal and myenteric ganglia (Figure 2A). To identify the total neural and glial content of ENCC-HIO-TESI, cross-sections of implants were imaged and the area of positive staining as a percent of the total tissue area per section for TUJ1, SMA, GFAP, and S100β was calculated and compared with 17-week-old human fetal ileum (Figure S1). ENCC-HIO-TESI demonstrated a similar area of TUJ1 (4.52% ± 4.67% versus 6.19% ± 2.45%), SMA (16.52% ± 10.42% versus 15.01% ± 2.35%), S100β (3.68% ± 1.57% versus 4.33% ± 4.25%), and a lesser number of GFAP (2.30% ± 1.07% versus 5.31% ± 3.79%) compared with 17-week-old fetal human ileum ($p < 0.05$) (Figure S1).

HIOs develop intrinsic pacemaker cells similar to native intestine, known as the interstitial cells of Cajal (ICCs), which are responsible for autonomic rhythmicity and are found in the submucosal and inter/intramuscular layers (Lee et al., 2007). We evaluated for the presence of

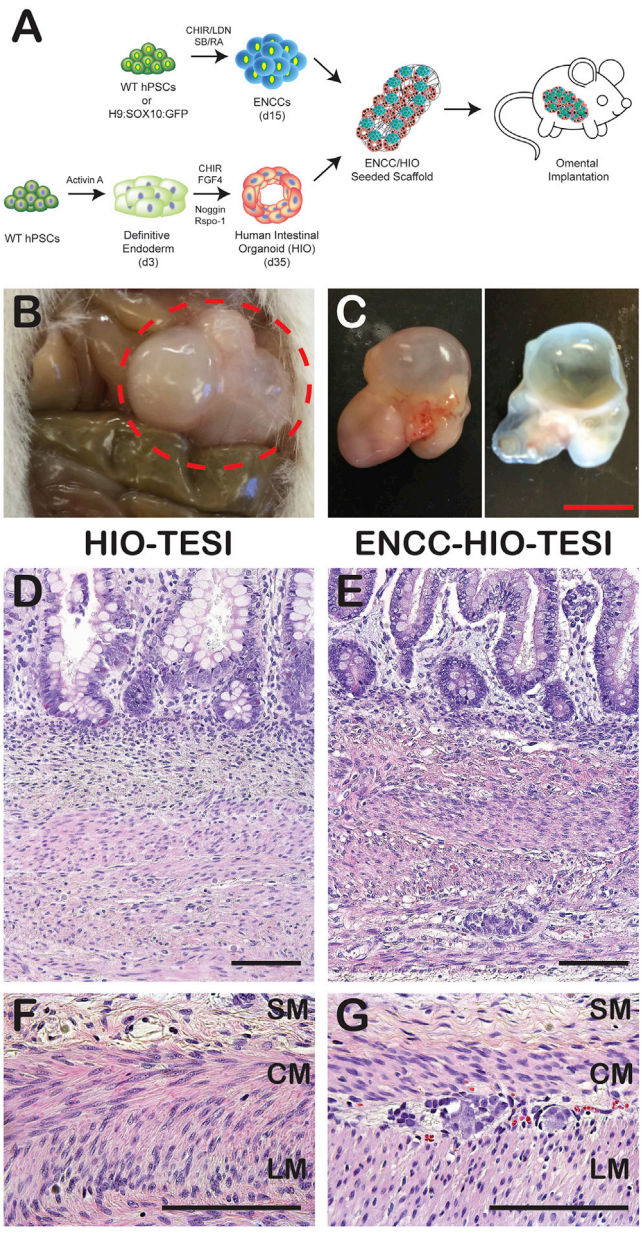

Figure 1. Generation of Human Intestinal Organoid-Derived Tissue-Engineered Small Intestine with an Enteric Nervous System

(A) Schematic of co-implantation of ENCCs into developing HIO-TESI to establish ENCC-HIO-TESI. Briefly, unmodified (wild-type [WT]) hPSCs were treated with defined factors as described previously to produce HIOs (Spence et al., 2011). Independently, unmodified WT hPSCs or H9::SOX10:GFP were treated as described previously until day 11 to ENCCs (Fattahi et al., 2016). Unsorted ENCCs were transferred into ultra-low attachment plates and allowed to form neurospheres for an additional 4 days. PGA/PLLA scaffolds were seeded with 4–6 HIOs (day 35 of differentiation) and 40–60 unsorted ENCC neurospheres (day 15 of differentiation), placed into the omentum of irradiated NOD/SCID mice, and allowed to mature for 3 months prior to explantation; n = 22.

(B) A mature ENCC-HIO-TESI *in vivo* implant (red dashed circle) within an NOD/SCID mouse.

(C) Whole explanted ENCC-HIO-TESI (left) and cross-section with prominent lumen visible after 10% buffered formalin fixation (right). Scale bar, 2.5 mm.

(D) H&E staining of control HIO-TESI demonstrating development of villus and crypt-like structures and underlying mesenchyme without ENS elements.

(E) H&E staining of ENCC-HIO-TESI restores mature ganglia and neurons within the submucosa.

(F) Higher-magnification H&E of control HIO-TESI demonstrate no ganglia within the submucosa (SM) or between the circular muscle (CM) and longitudinal muscle (LM) where the myenteric plexus arises.

(G) H&E staining reveals establishment of mature ganglia within the myenteric plexus of ENCC-HIO-TESI.

Scale bars in (D–G), 100 μm.

C-KIT-positive ICCs in ENCC-HIO-TESI and demonstrated that they closely associate with neurons in the myenteric plexus, similar to human fetal intestine. In HIO-TESI without ENCC supplementation, however, C-KIT-positive ICCs are randomly distributed within the myenteric layers (Figure 2B).

Human ENCC Supplementation Repopulates Enteric Ganglia and Excitatory, Inhibitory, and Sensory Neurons in ENCC-HIO-TESI

After successfully demonstrating neuronal and glial engraftment in ENCC-HIO-TESI, we further evaluated for retention of ENCC markers and neuronal subtypes. We identified well-organized PHOX2B and TRKC/RET/EDNRB triple-positive ganglia throughout the submucosal and myenteric plexuses similar to human fetal intestine (Figure 3A). The ENS contains numerous unique subtypes of neurons with distinct functions, electrophysiological properties, and neurotransmitter expression (Furness, 2012). Myenteric neurons include excitatory and inhibitory motor neurons, descending and ascending interneurons, and intrinsic primary sensory neurons (Costa et al., 2000). We identified excitatory neurons (CHAT/TUJ1) and sensory neurons (5-HT/TUJ1) in ENCC-HIO-TESI (Figure 3B). We also observed calbindin/TUJ1 and calretinin/TUJ1 double-positive neurons (Figure 3B). Although a majority of calretinin-positive neurons are excitatory motor neurons, a small number represent intrinsic sensory neurons of the ENS (Kunze and Furness, 1999; Qu et al., 2008).

Inhibitory neurons within the myenteric plexus and muscle fibers of the human small intestine (SI) and colon contain neuronal nitric oxide synthase (nNOS), which is the predominant isoform of NOS in the ENS and an integral component of the intestinal peristaltic reflex, secretion, digestion, absorption, and elimination. Production of nitric oxide results in relaxation of smooth muscle and

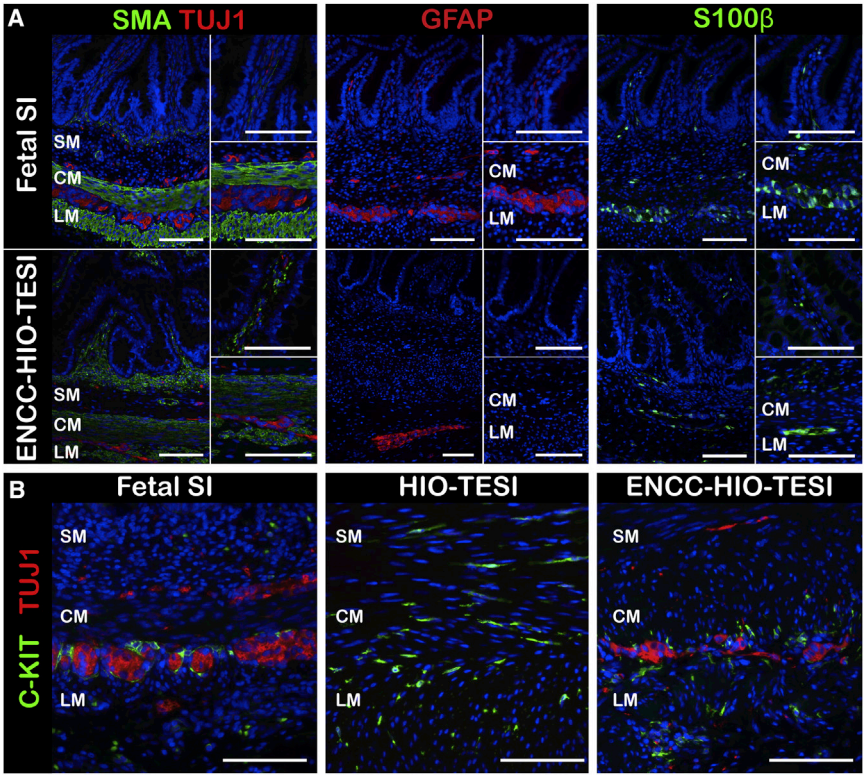

Figure 2. ENCC Supplementation Restores Enteric Neurons and Glia and Their Association with ICCs in ENCC-HIO-TESI

(A) Immunofluorescent stains of human fetal ileum (upper row) and ENCC-HIO-TESI (bottom row). Human fetal intestine identifies organized TUJ1-positive neurons (red) within the submucosal and myenteric plexuses with extension into the tips of the villi and well-developed muscularis mucosae and propria (SMA, green, left panel). GFAP-positive (red) and S100β-positive (green) glia were also identified within the submucosal and myenteric plexuses (middle and right panels). In the bottom row, ENCC-HIO-TESI reveals a well-organized muscularis mucosa and propria (SMA, green) with neurons (TUJ1, red) present within the submucosa and myenteric layers (bottom row, left panel). TUJ1-positive (red) ganglia are present within the villi (upper inset) and the location of the myenteric plexus (lower inset). GFAP-positive (red) glia were present in ENCC-HIO-TESI (middle panel); however, they were absent in villi (upper inset) and within the myenteric plexus (lower inset). S100β-positive (green) glial cells are identified within the submucosal and myenteric plexuses of ENCC-HIO-TESI (right panel).

(B) C-KIT-positive (green) ICCs are present within the smooth muscle of human fetal small intestine (left panel), HIO-TESI (middle panel), and ENCC-HIO-TESI (right panel). C-KIT-positive ICCs are highly associated with TUJ1-positive ganglia (red) in human fetal small intestine and ENCC-HIO-TESI; nuclei are labeled with DAPI (blue).

Scale bars, 100 μm (n = 11).

controls the opening of sphincters, and mediates receptive and accommodative relaxation (Beck et al., 2009; Takahashi, 2003; Timmermans et al., 1994). It has been shown that the functional obstruction seen in HD patients may be caused by an inability to relax enteric smooth muscle (Furness, 2012). Co-implantation of ENCCs into developing HIO-TESI establishes inhibitory nNOS/TUJ1 double-positive neurons within the myenteric plexus (Figure 4B). Taken together, these data identify the establishment of enteric ganglia within the submucosal and myenteric plexuses and engraftment of excitatory, inhibitory, and sensory neurons required for restoration of ENS function in ENCC-HIO-TESI.

Engrafted ENCCs Establish Dense Connectivity within the Muscularis Propria and Form Synaptic Connections with the EECs of the Luminal Epithelium

Establishing appropriate restoration of the location and subtypes of ENS neurons and glia, we next sought to evaluate the extent of neuronal projections within the smooth muscle and to epithelial cells of the villus. Light-sheet microscopy identified the presence of dense TUJ1-positive axonal projections throughout the smooth muscle (SMA) in ENCC-HIO-TESI, whereas HIO-TESI lacked TUJ1-positive neurons (Figure 4A). Intraluminal sensory signaling from enteroendocrine cells (EECs) is critical in regulating numerous processes in the gastrointestinal tract, including release of digestive enzymes, activation of nutrient and fluid transporters, and regulation of immune responses (Furness et al., 2013). The propagation of these signals occurs through connections between EEC and underlying enteric neurons (Bohorquez et al., 2015). Evaluation by 3D confocal microscopy demonstrated TUJ1-positive axonal projections to EECs cell bodies, suggesting the establishment of neuroepithelial synaptic connections (Figure 4B).

Neuronal-Dependent Contractility and Relaxation Is Restored in ENCC-HIO-TESI

The nervous system control of the gastrointestinal tract is comprised of intrinsic neurons of the ENS and extrinsic sympathetic, parasympathetic, and sensory neurons of the CNS that regulate a host of processes, including

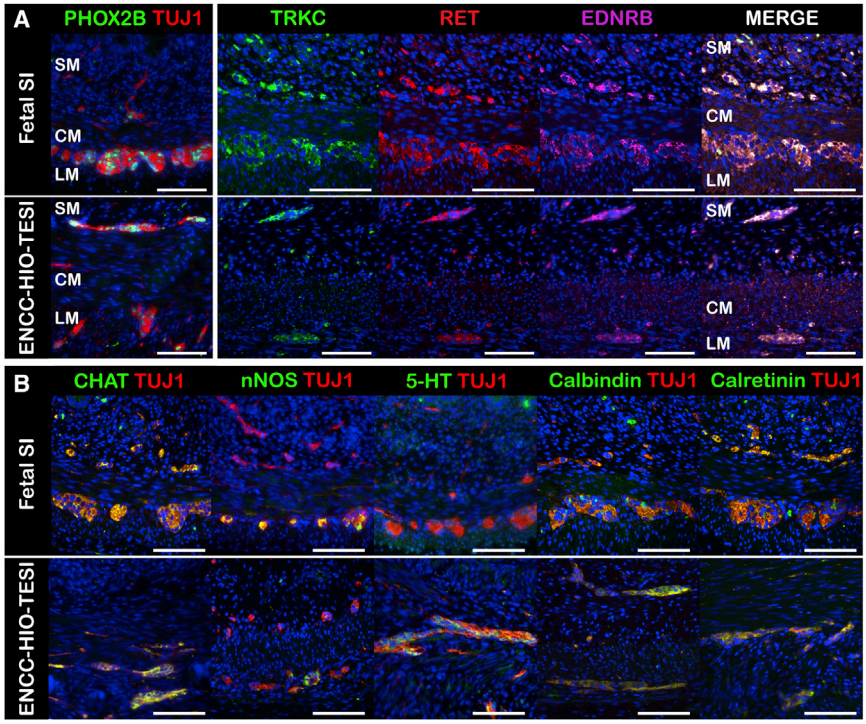

Figure 3. Vagal-Specific Ganglia and a Wide Array of Neuronal Subtypes Are Present in ENCC-HIO-TESI

Immunofluorescent staining of human fetal ileum and ENCC-HIO-TESI.

(A) TUJ1-positive submucosal and myenteric ganglia express vagal and enteric neural crest cell markers PHOX2B and TRKC/RET/EDNRB; submucosa (SM), circular muscle (CM), longitudinal muscle (LM). Scale bars, 100 μm (n = 6).

(B) Various subclasses of enteric neurons were identified, including excitatory (CHAT/TUJ1), inhibitory (nNOS/TUJ1), and sensory neurons (5-HT/TUJ1). Calbindin- and calretinin-positive neurons were also restored in ENCC-HIO-TESI; nuclei are labeled with DAPI (blue). Scale bars, 100 μm (n = 11).

peristalsis, migrating motor complexes, segmentation, mixing, digestion, absorption, secretion, excretion, and barrier defense (Furness, 2012; Furness et al., 2014; Uesaka et al., 2016). However, studies of externally denervated intestine have demonstrated that the ENS can autonomously regulate motility (Furness et al., 1995). To test for restoration of mechanical contraction in ENCC-HIO-TESI, implants were harvested and underwent live-video imaging. HIO-TESI demonstrate spontaneous contractility even without supplementation with ENCCs due to autonomic firing of ICCs (Movie S1). Upon treatment of HIO-TESI with methylene blue, a known inhibitor of ICCs (Liu et al., 1994), a marked reduction in contractility is observed (Movie S2). Similar to HIO-TESI, ENCC-HIO-TESI also contracts after explantation (Movie S3). However, treatment with methylene blue failed to completely block contractility in ENCC-HIO-TESI (Movie S4). Upon treating ENCC-HIO-TESI with tetrodotoxin (TTX), contractility was inhibited, suggesting that the enduring contraction and relaxation following methylene blue treatment is neuron dependent and independent of ICCs (Movie S5).

Transcriptional Profiling of ENCC Supplementation in Developing HIO-TESI

To explore the unique changes in gene expression between ENCC-HIO-TESI and HIO-TESI, we performed RNA-seq on three ENCC-HIO-TESI and three HIO-TESI samples. In brief, the isolated RNA was sequenced, aligned to the human genome, and processed for the removal of unwanted variation (RUV) with empirical normalization (Figures S3A–S3F). Principle-component analysis plots display the distribution of each sample before and after normalization of the RNA-seq data (Figures S3B and S3E). Volcano plots of the data after RUV processing demonstrated 849 differentially expressed (DE) genes with an false discovery rate (FDR) value <0.05 in ENCC-HIO-TESI compared with HIO-TESI (Figure S3F). Of the 849 DE genes, 503 were shown to be upregulated and 72 downregulated with a $\log_2$ fold change >2 (Figure S3F).

From our data, we observed significant DE genes known to be related to the ENS (PHOX2B, PHOX2A, FOXD3, and PAX3), glial cells (GFAP and S100B), and neurotransmission (NOS1, VIP, HTR2A, HTR2C, GRM8, and GRIK3) (Table 1). Gene ontology (GO) pathway analysis of the over-represented pathways in ENCC-HIO-TESI-containing DE genes included upregulated pathways integral to nervous system development, neurological system processes, synaptic signaling, and vasculature development, and downregulated pathways involved in immune system responses (Figure 5). Importantly, we observed the upregulation of genes within GO pathways involved in interneuron migration and differentiation as well as neuromuscular processes, synaptic transmission, ion transport, and axonogenesis (Figure 5A).

To determine if ENCC supplementation *in vivo* altered the development of intestinal stem and progenitor cells

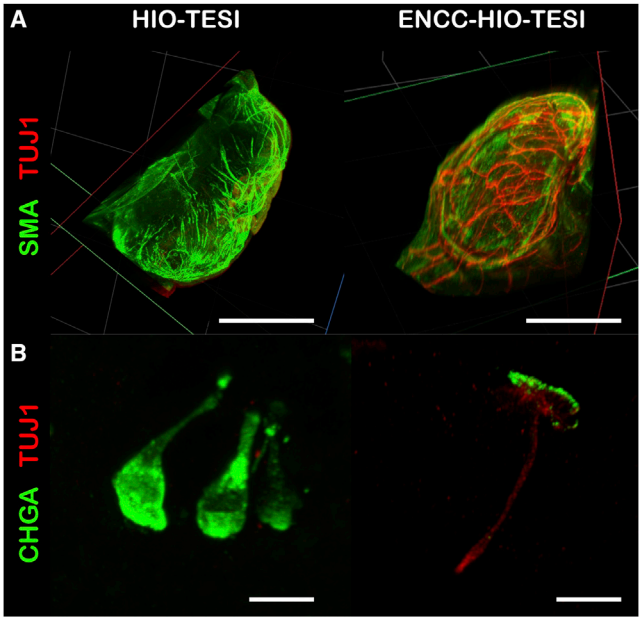

Figure 4. Implanted ENCCs Develop Robust Axonal Projection within the Muscularis Propria and Synapse to EECs of ENCC-HIO-TESI

(A) Light-sheet microscopy of HIO-TESI and ENCC-HIO-TESI. Maximal intensity projections of HIO-TESI demonstrate the absence of TUJ1-positive neurons (red) within the muscularis propria (SMA, green). Prominent TUJ1-positive neuronal axons (red) are identified traversing the smooth muscle in ENCC-HIO-TESI (SMA, green). Scale bars, 3 mm (n = 5).

(B) Confocal microscopy identified enteroendocrine cells (CHGA, green) within HIO-TESI and ENCC-HIO-TESI. A TUJ1-positive neuronal axon forms synaptic connections with the bottom of a CHGA-positive enteroendocrine cell. Scale bars, 10 μm (n = 5).

or differentiated epithelial cell types, selected genes of interest were evaluated, and heatmaps based on gene reads per kilobase per million mapped reads were generated (Figure 6F). We did not detect significant changes in intestinal stem and progenitor cell genes or absorptive enterocytes in ENCC-HIO-TESI compared with HIO-TESI; however, secretory cell lineages were altered, including a significant upregulation in the Paneth cell gene LYZ and a concomitant decrease in enteroendocrine genes, GCG and NTS, and in several goblet cell genes, including GUCA2A, MUC2, TFF3, RETNLB, and FCGBP (Figures 6A–6E).

ENCC Supplementation Has Distinct Effects on Transcriptome Profiles of Intestinal Stem and Differentiated Epithelial Cell Types during *In Vivo* versus *In Vitro* HIO Development

Diverse methods are proven to derive human ENCCs (Fattahi et al., 2016; Huang et al., 2016; Workman et al., 2017) and enteric neurospheres from primary adult intestinal tissues (Hetz et al., 2014; Metzger et al., 2009a; Wilkinson et al., 2015), with the potential for treatment of enteric neuropathies. A recent publication by Workman et al. identified the effects of ENCC supplementation in *in vitro* co-cultured hPSC-derived ENCCs with HIOs (HIO + ENS) and RNA-seq was performed to evaluate transcriptome changes after ENCC supplementation (Workman et al., 2017). Comparisons of *in vivo* versus *in vitro* methods of ENCC supplementation might reveal key steps for the successful reintegration of ENS components in tissue-engineered organs. Therefore, we compared the transcriptomic profiles of ENCC-HIO-TESI generated through our *in vivo* supplementation method and HIO + ENS generated via the Workman et al. *in vitro* method.

Applying stringent criteria for identifying DE genes (FDR value <0.05 compared with uncorrected p value < 0.05 as employed by Workman et al.), evaluation of RNA-seq data from Workman et al. demonstrated DE of 1910 genes with an FDR <0.05 (Table S4). Of the 1,910 DE genes, 1,026 genes were upregulated ($\log_2$ fold change >2) and 232 genes were downregulated ($\log_2$ fold change < −2) between *in vitro* HIO + ENS and HIOs (Table S4). Comparing *in vivo* ENCC-HIO-TESI to *in vitro* HIO + ENS by the same criteria, we identified 192 shared DE genes (Table S5), 657 DE genes altered in ENCC-HIO-TESI alone (Table S6), and 1,718 expressed solely in HIO + ENS (Table S7). Of the 192 shared DE genes, several neural crest cell and ENS genes were upregulated, including PHOX2B, PHOX2A, PAX3, FOXD3, SIX3, ZIC1, ZIC2, ZIC3, ZIC4, and ZIC5 (Table S5). DE genes in ENCC-HIO-TESI alone included markers of gliogenesis and those involved in neurotransmission (Tables 1 and S6).

To analyze whether neural supplementation *in vivo* and *in vitro* differentially affected epithelial cells in developing constructs, the same selected genes of interest in stem cells, enterocytes, EEC, Paneth cells, and goblet cells shown in Figure 6 were examined in the Workman et al. RNA-seq dataset. Compared with *in vivo* ENCC-HIO-TESI, in which there were no appreciable changes in intestinal stem or progenitor cell gene expression, analysis of *in vitro* HIO + ENS revealed differential gene expression in intestinal stem and progenitor cell markers and selected epithelial cell populations. Applying rigorous criteria of FDR < 0.05 while evaluating several known stem cell-specific genes, we identified significant downregulation of SMOC2 and upregulation of HOPX, ATOH1, DCLK1, MSI1, and TNFRSF19 in *in vitro* HIO + ENS (Table S4). In evaluating mature epithelial cell types, no significant differences in absorptive enterocyte markers were seen in *in vivo* ENCC-HIO-TESI (Figure 6B; Table S3), while a significant decrease of SLC9A9 was demonstrated *in vitro* HIO + ENS (Table S4). *In vivo* ENCC-HIO-TESI showed

Table 1. Differential Expression of Genes Important in Development and Function of the Neural Crest Cells and the Enteric Nervous System

Pathway	Gene Name	Log_2 Fold Changes
Neural crest cell development	ALX1, FOLR1, NKX6-1, NKX6-2, NKX6-3, OTX2, PAX3, PHOX2A, PHOX2B, PITX2, SIX3, SPINK1, WIF1, ZIC1, ZIC2, ZIC3, ZIC4, ZIC5	−2.94, 4.22, 7.64, 3.86, 5.73, 10.0, 3.71, 3.88, 5.95, −1.28, 7.75, 1.47, 0.93, 7.24, 7.64, 7.52, 10.23, 10.23
Gliogenesis	CDH2, DLX2, DNER, GFAP, NKX6-1, NKX6-2, NR2E1, OLIG1, PENK, PHOX2B, RELN, S100B, TP73, TRPC4	1.17, 3.92, 2.83, 6.56, 7.64, 3.86, 6.89, 5.90, 1.67, 5.95, 4.57, 4.34, 1.80, 1.40
Excitatory neuron signaling	CHRNA3, CUX2, DLG4, RELN, RGS8	1.76, 2.15, 0.80, 4.57, 4.79
Dopamine signaling	ADCY8, GRIN2B, NOS1, RGS8	3.47, 3.72, 3.99, 4.79
GABA signaling	GABRE, GABBR1	1.20, 0.81
Glutamate signaling	CACNG8, DLG4, GRIA1, GRIK3, GRIN2B, GRM8, NECAB2	2.31, 0.80, 1.46, 4.24, 3.72, 4.62, 2.52
Serotonin signaling	CHRNA3, HTR2A, HTR2C, SERTM1	1.76, 1.71, 10.73, 6.81

the significant upregulation of Paneth cell gene LYZ and the significant downregulation of EEC genes GCG and NTS (Figures 6C and 6D; Table S3). Analysis of *in vitro* HIO + ENS demonstrated a significant increase in a subset of secretory cell genes, including EEC genes CHGB, ARX, NEUROG3, and PAX6, as well as Paneth cell gene DLL1 (Table S4). In *in vivo* ENCC-HIO-TESI, we observed significant decreases in several goblet cell genes (Figure 6E); however, in *in vitro* HIO + ENS by Workman et al., no significant changes were noted in the goblet cell genes examined.

ENCC Effects on the Gastrointestinal Tissue-Specific Transcriptome during *In Vivo* and *In Vitro* Development of HIOs

We next sought to identify whether genes enriched in the adult human gastrointestinal tract were altered in response to ENCC supplementation. Gremel et al. (2015) performed RNA-seq analysis of adult human stomach, duodenum, jejunum/ileum, and colon specimens, and compared their gene expression with 23 other non-gastrointestinal tract tissues. They identified genes enriched or elevated in expression in various anatomical locations along the gastrointestinal tract, including 180 SI-specific genes incorporating both duodenum and jejunum/ileum genes, 80 colon-specific genes, and 52 genes commonly expressed in both SI and colon (Gremel et al., 2015). To establish any additional gastrointestinal tissue specificity imparted to HIO-TESI by supplementation with ENCCs, we first surveyed our *in vivo* RNA-seq data for the three sets of gastrointestinal tissue-specific genes identified by Gremel et al. We also compared this list of tissue-specific genes from Gremel et al. to the Workman et al. RNA-seq data to identify if ENCCs affected HIOs similarly *in vitro*.

A subset of the genes specific to SI, colon, and colon/SI were differentially expressed within ENCC-HIO-TESI and/or HIO + ENS (Figures 6F and 6G). Nine out of the total 559 (1.61%) downregulated genes within the Workman et al. dataset represent SI-specific genes, while 4 of 559 (0.72%) downregulated genes represent colon- or colon/SI-specific genes. Comparing ENCC-HIO-TESI to HIO-TESI, 4 out of the total 173 (2.3%) downregulated genes in our data were SI specific, 9 of 173 (5.2%) downregulated genes were colon/SI specific, and 23 of 173 (13.3%) downregulated genes were colon specific. Of these downregulated genes, certain SI-, colon-, and colon/SI-specific genes were DE in both datasets, including MT1H (SI specific), TMEM171 (colon specific), and PHGR1 (colon/SI specific). In addition, three SI-specific genes were upregulated within HIO + ENS, including SLC17A8, which was also upregulated in ENCC-HIO-TESI.

DISCUSSION

Human ENCC neurosphere co-implantation into HIO-TESI restores an ENS cytoarchitecture nearly identical to native intestine. Our approach restores the myenteric and submucosal plexuses, and establishes diverse enteric neuronal and glial subclasses (Figures 2A, 3A, and 3B). Light-sheet and confocal microscopy demonstrated a complex myenteric plexus and establishment of synaptic connections with EECs, potentially restoring neurotransmission from luminal ECCs and underlying enteric neurons, a feature not seen in HIO-TESI or in previous *in vivo* models (Workman et al., 2017). TESI developed by this method (both with and without ENCC supplementation) possesses an intrinsic ICC-dependent contractile ability (Movies S1 and S3). However, methylene blue treatment, which

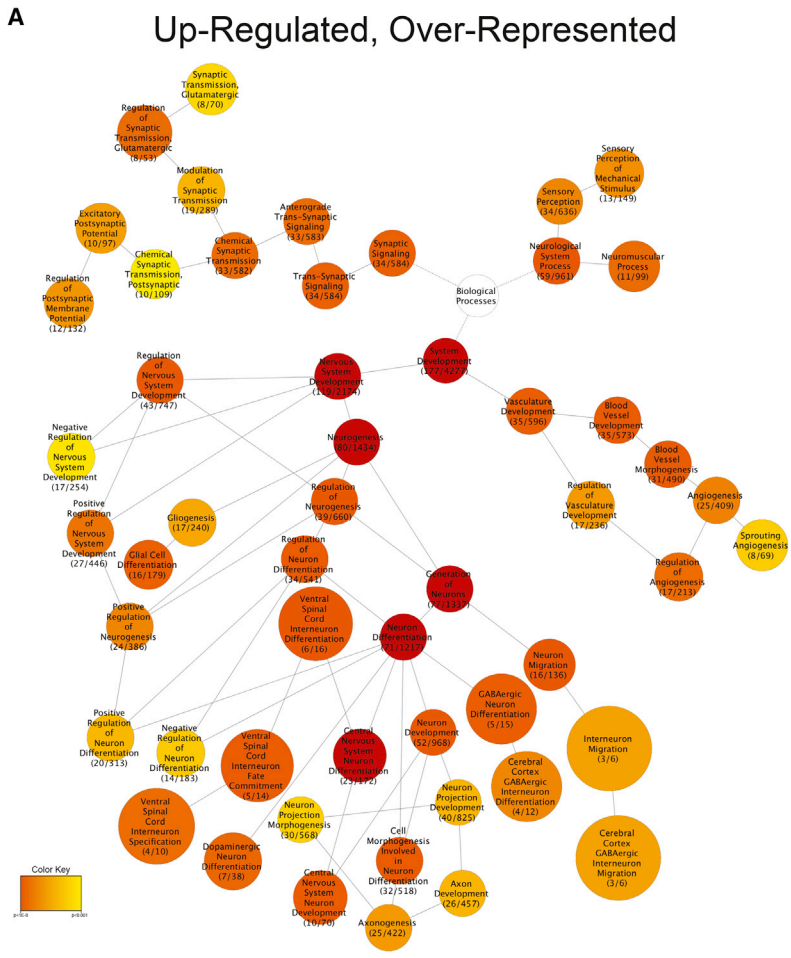

Figure 5. Gene Ontology Pathways Over-Represented in ENCC-HIO-TESI

Using Cytoscape, hierarchical maps of a subset of GO terms containing genes over-represented among the differentially expressed genes in ENCC-HIO-TESI were constructed. p Values range from 1×10^{-8} (orange) to 0.001 (yellow), and range in color as shown in the color key. GO terms whose p values were less than 1×10^{-8} are displayed in red, while those whose p values exceed 0.001 are colored in white and are not deemed significantly over-represented. The size of circular nodes in the trees, each of which designates an individual GO term, represents the percentage of the total genes in that term that are (A) up- or (B) downregulated. Therefore, bigger nodes reflect that a larger proportion of genes in the GO term are over-represented. The fraction of genes present in our data is included, along with the name of each GO term, on each node of the charts. (A) A subset of GO terms containing genes that are upregulated (positive logarithmic fold change) and over-represented in ENCC-HIO-TESI. The lines connecting nodes are either solid, indicating a direct parent-child relationship as defined by the GO Consortium, or dashed, indicating an indirect relationship from a more general node to a more specific node. (B) A subset of GO terms that are significantly downregulated (negative logarithmic fold change) and over-represented in ENCC-HIO-TESI. Some of these GO terms are not significantly over-represented in our dataset (white nodes), but are included for completion of the tree.

inhibits ICC function in the SI (Liu et al., 1994), abolished contractility in HIO-TESI after 4 hr, whereas mechanical contractility persisted in ENCC-HIO-TESI (Movies S2 and S4). Further treatment of ENCC-HIO-TESI with the neuronal inhibitor TTX significantly impaired residual contractility, suggesting that the contractility observed is neuron dependent and ICC independent (Movie S5). Taken together, these data demonstrate functional integration of enteric neurons in ENCC-HIO-TESI.

Workman et al. recently reported an alternative method for the derivation of ENCCs from hPSCs, with the ability to restore ENS elements in HIOs *in vitro* and *in vivo* (Workman et al., 2017). The differences in ENCC differentiation and approaches to restoring ENS in HIOs between these two protocols result in the divergent expression of neuronal cell types and ENS functional maturity. For instance, CHAT-positive neurons appeared early during *in vitro* experiments of HIO + ENS, but were absent after *in vivo* growth in Workman et al. Restoration of CHAT-positive motor neurons and ascending interneurons is critical for the maintenance of peristalsis and segmentation (Burns et al., 2009; Kunze and Furness, 1999). Our method maintains CHAT-positive neuronal cell populations *in vitro* (Figure S2) and *in vivo* (Figure 4A). In addition, our method establishes neuronal connections with EEC (Figure 4B), which failed to form in previous studies (Workman et al., 2017). EECs express cellular elements necessary for neurotransmission and, in the mature intestine, serve as part of a neuroepithelial circuit important in enteric sensory activity (Bohorquez et al., 2015). The synaptic connection of EECs and TUJ1-positive neurons in ENCC-HIO-TESI demonstrates the potential of this method to restore this critical neuroepithelial network. Overall, we demonstrate that our protocol involving early *in vivo* co-implantation of hPSC-derived ENCC neurospheres allows for functional integration and establishment of neuroepithelial connections that could be important for restoring luminal sensory function of ENCC-HIO-TESI.

The discordant findings between these two studies can be explained by differences in ENCC derivation, timing of implantation, and cell identity at time of implantation. Our approach involves the early *in vivo* co-implantation of HIOs with ENCC neurospheres after day 15 of ENCC differentiation, as opposed to culturing HIO + ENCC for 4 weeks *in vitro* prior to *in vivo* implantation, as reported by Workman et al. Our protocol features more defined media and small-molecule-driven differentiation with longer exposure to retinoic acid (5 days compared with 2 days), which may prime ENCCs to differentiate earlier and more robustly. In addition, the implantation of whole neurospheres, as performed here instead of dissociated single cells by Workman et al., may account for the discordance in functional integration that is observed between the two methods. Early transplantation and injection of intact neurospheres versus single cells have been suggested to improve survival and engraftment rates (Johann et al., 2007). Maintenance of cell-cell interactions in developing neurospheres could provide a better environment for engraftment and integration, as culturing neurospheres in 3D versus monolayer culture promotes a more homogeneous expression of neural progenitor cell markers and increases their differentiation potential (Zhou et al., 2016). These differences in methodology appear to have a profound effect on the subsequent ability of ENCCs to engraft, differentiate, and persist *in vivo*.

Given the potential for ENCCs and primary enteric neurosphere supplementation for the future treatment of enteric neuropathies, directed studies comparing *in vitro* and *in vivo* maturation of ENCCs will begin to answer questions regarding the importance of timing of implantation with regard to survival, proliferation, migration, differentiation, and functional integration into recipient tissues (Burns et al., 2016). RNA-seq analysis of *in vivo* versus *in vitro* methods of ENCC supplementation evaluated with the same normalization methods and analysis stringency reveals 657 DE genes unique to ENCC-HIO-TESI, 1,718 DE genes unique to HIO + ENS, and 192 DE genes common to both preparations, many of which were integral to neural crest cell and ENS development (Tables S5, S6, and S7). Workman et al. (2017) evaluated the effects of ENCC supplementation on the expression of stem cell genes and a variety of epithelial cell genes, suggesting alterations within all classes. We did not observe differential gene expression in stem cell genes or absorptive lineages in *in vivo* ENCC-HIO-TESI compared with HIO-TESI. However, we do identify significant downregulation in the goblet cell lineage, which was not observed under *in vitro* conditions (Figure 6E; Table S3).

In addition, an analysis of the expression of gastrointestinal tissue-specific genes demonstrated that, overall, the addition of ENCCs further patterns HIOs toward a small intestinal fate upon *in vivo* co-implantation. More colon- and colon/SI-specific genes are significantly downregulated in *in vivo* ENCC-HIO-TESI than in *in vitro* HIO + ENS, while more SI-specific genes are significantly downregulated in *in vitro* HIO + ENS than in *in vivo* ENCC-HIO-TESI (Figures 6F and 6G). This may indicate that ENCC supplementation in the *in vivo* environment develops tissue specificity by promoting intestinal proximalization away from a colonic fate and toward SI. Vagal ENCCs are known to migrate and differentiate caudally from foregut to hindgut, first populating the regions where myenteric plexuses will form, followed by the colonization of the submucosa (Burns and Douarin, 1998). In studies of ENCC migration in avian models, it has been shown that, while vagal neural crest cells contribute the vast majority of enteric ganglia, sacral

(legend on next page)

neural crest cells have a distinct role in patterning the distal gut (Burns and Douarin, 1998; Goldstein and Nagy, 2008). Given the observations in this paper, perhaps supplementation of HIOs with sacral ENCCs will promote a more colonic phenotype and should be explored to further delineate the effects of specific subpopulations of ENCCs on gastrointestinal tract development.

Taken together, these data support an improved strategy for restoring and maturing a human ENS in ENCC-HIO-TESI and establishing neuron-dependent motility through ENCC supplementation. Ultimately, the protocol described here demonstrates the potential for hPSC-derived ENCCs as a future therapeutic source for treating human enteric neuropathies. The advances described in this paper represent necessary steps toward establishing tissue-engineering strategies for future human therapies in the treatment of intestinal loss, failure, or enteric neuropathies.

EXPERIMENTAL PROCEDURES

Maintenance of hPSCs and Generation of HIOs and ENCCs

The University of Southern California and Children's Hospital Los Angeles Stem Cell Research Oversight committee approved all work using hPSCs. Human ES cell line H9 (WA-09), H9::SOX10::GFP, and human iPSC cell line WTC (Bruce Conklin) were maintained on Matrigel (BD Biosciences, 354234) in mTeSR (STEMCELL Technologies, 05850). HIOs were generated as described previously to day 28 to 35 of age (McCracken et al., 2011; Spence et al., 2011). ENCCs were generated up to day 11 as described previously (Fattahi et al., 2016). On day 11, unsorted ENCCs were aggregated into 3D spheroids in ultra-low attachment multiwell plates (Corning Life Sciences, CLS3471) and cultured in neurobasal medium supplemented with N2/B27 containing 3 μM CHIR99021 and 10 nM FGF2 (R&D Systems, 233-FB-001MG/CF) for an additional 4 days. For *in vitro* long-term culture, plated ENCCs were cultured as described previously (Fattahi et al., 2016).

Generation of HIO-Derived Tissue-Engineered SI with and without ENCCs

All animal protocols were reviewed and approved by the Institutional Animal Care and Use committee of the Children's Hospital Los Angeles (CHLA). Hosts for HIO-TESI and ENCC-HIO-TESI implantation were immunosuppressed NOD/SCID gamma mice (Jackson Laboratory). Procedure for scaffold preparation and surgical implantation can be viewed in our laboratory's previous JOVE publication (Barthel et al., 2012b). Six HIOs (days 28–35 of differentiation) and 40–60 unsorted ENCC neurospheres (day 15 of differentiation) were mixed and seeded onto biodegradable scaffolds, wrapped in the omentum of adult NOD/SCID mice, and allowed to mature for 3 months before surgical removal to create ENCC-HIO-TESI (Figure 1A). HIO-TESI was generated without supplementation of ENCC as published previously (Finkbeiner et al., 2015). At 3 months, implants were excised, fixed in 10% buffered formalin, and embedded into paraffin blocks for histological analysis.

Histology, Immunofluorescence, and Image Quantification

Human fetal ileum samples were obtained with the approval of the Institutional Review Board of CHLA and the University of Southern California. Consent was obtained prior to tissue donation. Human fetal ileum and implanted constructs were formalin-fixed, embedded in paraffin, and sectioned at 5 μm. H&E staining was performed on the sectioned tissue. The slides were imaged at 20× magnification on a Leica DM 1000 bright-field microscope (Leica, Wetzlar, Germany).

In preparation for immunofluorescence, slides were deparaffinized and rehydrated before undergoing antigen retrieval. Samples underwent blocking for 30 min at room temperature. Primary antibodies (Table S1) were diluted in universal blocking solution and placed on tissue overnight at 4°C. Tissues were washed in PBS-Tween, and appropriate secondary antibodies diluted in PBS with 0.05% Tween (Table S2) were applied to tissue for 1 hr at room temperature. For quantification of TUJ1, SMA, S100β, and GFAP, positive immunostaining was identified within each sample and divided by the total area of the cross-section to identify total percentage of fluorescence within the samples using ImageJ (Schneider et al., 2012).

Tissue Clearing and Fluorescence Microscopy

HIO-TESI and ENCC-HIO-TESI implants were removed at 3 months and fixed overnight. Samples were dehydrated and incubated at room temperature overnight in 2:1:3 MeOH:DMSO:30% H_2O_2. The following day, samples were brought to −80°C for 1 hr and then warmed to room temperature. Samples were rehydrated and blocked in 3% BSA in Tris-buffered saline-Tween with 0.01% NaAz for 24 hr. The following day, samples were incubated with the primary antibody diluted in blocking solution for 72 hr. The secondary antibody, diluted in blocking solution, was then incubated for 24 hr. Following secondary antibody incubation, samples were dehydrated and then cleared in 1:2 benzyl alcohol:benzyl benzoate for more than 24 hr until imaging. Light-sheet microscopy was performed on a LaVision BioTec Ultramicroscope UM-0078 (LaVision BioTec, Bielefeld, Germany). Images were processed on arivis Vision4D software (arivis AG, Munich, Germany).

Figure 6. Genome-wide Analysis of ENCC-HIO-TESI Identifies Alterations in Gastrointestinal Tract Maturity and Intestinal Epithelial Cell Types

(A–E) Heatmaps of selected genes of interest were created for intestinal stem/progenitor cells, enterocytes, enteroendocrine cells, Paneth cells, and goblet cells, respectively.

(F–G) DE genes specific or enriched in colon, colon/small intestine (C/SI), and small intestine were identified in (F) *in vivo* ENCC-HIO-TESI and (G) *in vitro* HIO + ENS (n = 3 samples per condition).

Confocal Images were obtained on a Zeiss LSM700 Confocal System mounted on an AxioObserver.Z1 microscope (Carl Zeiss, Thornwood, NY).

Time-Lapse Video Microscopy of Mechanical Contractility

HIO-TESI and ENCC-HIO-TESI were explanted and allowed to equilibrate for 1hr in FluoroBrite DMEM (Thermo Fisher Scientific, A18967-01) at 37°C, and imaged using a Leica MZ12.5 Steromicroscope with a Leica MC170 HD Camera. Explants were initially imaged to evaluate for spontaneous contractility. In samples where spontaneous contractility was observed before and after intraluminal injection of FluroBrite DMEM, methylene blue (50 μM) was injected intraluminally, and whole explants were soaked for 4 hr prior to imaging to selectively inhibit contractility produced by ICCs (Liu et al., 1994). ENCC-HIO-TESI explants that retained contractility after methylene blue treatment were intraluminally injected and soaked with TTX (10 μM) for 4 hr. HIO-TESI and ENCC-HIO-TESI in control FluoroBrite DMEM without methylene blue or TTX treatment were imaged after 8 hr and demonstrated continued contractility *in vitro*. Videos were post-processed to 30× speed to visualize contractility. High-resolution videos can be viewed at https://figshare.com/s/6a70ff0256bf90300acb.

RNA-Seq and Analysis

Total RNA was extracted using the RNeasy Mini Kit (QIAGEN) and column purification with on-column DNase digestion (QIAGEN, Valencia, CA). RNA concentration was measured with NanoDrop (Thermo Fisher Scientific, Waltham, MA). cDNA libraries for RNA-seq were constructed from three HIO-TESI and ENCC-HIO-TESI cellular preparations by Quickbiology (www.quickbiology.com, Pasadena, CA). Before library construction, samples were spiked with Ex-Fold External RNA Controls Consortium controls (Ambion, Foster City, CA). Libraries then underwent deep sequencing to 50 million reads of length 140 base pairs, paired end. Descriptive methods for RNA-seq analysis can be found in the supplemental text.

ACCESSION NUMBERS

RNA-seq raw data and processed data were deposited in the National Center for Biotechnology Information Gene Expression Omnibus. They can be accessed through accession number GEO: GSE99317.

SUPPLEMENTAL INFORMATION

Supplemental Information includes Supplemental Experimental Procedures, three figures, seven tables, and five movies and can be found with this article online at http://dx.doi.org/10.1016/j.stemcr.2017.07.017.

AUTHOR CONTRIBUTIONS

Study Concept and Design, C.R.S. and T.C.G.; Acquisition of Data, C.R.S., K.L.F., M.T., I.H., S.H., M.T., B.G., and X.H.; Analysis and Interpretation of Data, C.R.S., K.L.F., M.T., I.H., J.R.S., and T.C.G.; Drafting of the Manuscript, C.R.S., K.L.F., and T.C.G.

ACKNOWLEDGMENTS

This work is supported by the California Institute of Regenerative Medicine (CIRM, TG2-01161 and RN3-06425). The authors would like to thank Narine Harutyunyan and Andrew Salas (CHLA Stem Cell Core), Esteban Fernandez, PhD (CHLA Microscopy Core), Aimin Li and Monica Mendez (CHLA Histology Core), and Krystal Arreola (CHLA Animal Facility), for their technical expertise. We thank Bruce Conklin, MD (J. David Gladstone Institutes) for providing the WTC hiPSC cell line and Gabsang Lee, PhD (Johns Hopkins University), for offering the modified H9::SOX10::GFP hESC cell line. Fetal tissue was received courtesy of Melissa Wilson, PhD (USC) and Rachel Steward, MD, MSc (Family Planning Associates). We are especially grateful to our patients and their families for supporting our research through tissue donation.

Received: January 2, 2017
Revised: July 20, 2017
Accepted: July 21, 2017
Published: August 10, 2017

REFERENCES

Barthel, E.R., Levin, D.E., Speer, A.L., Sala, F.G., Torashima, Y., Hou, X., and Grikscheit, T.C. (2012a). Human tissue-engineered colon forms from postnatal progenitor cells: an in vivo murine model. Regen. Med. *7*, 807–818.

Barthel, E.R., Speer, A.L., Levin, D.E., Sala, F.G., Hou, X., Torashima, Y., Wigfall, C.M., and Grikscheit, T.C. (2012b). Tissue engineering of the intestine in a murine model. J. Vis. Exp., e4279.

Beck, M., Schlabrakowski, A., Schrodl, F., Neuhuber, W., and Brehmer, A. (2009). ChAT and NOS in human myenteric neurons: co-existence and co-absence. Cell Tissue Res. *338*, 37–51.

Binder, E., Natarajan, D., Cooper, J., Kronfli, R., Cananzi, M., Delalande, J.-M., McCann, C., Burns, A.J., and Thapar, N. (2015). Enteric neurospheres are not specific to neural crest cultures: implications for neural stem cell therapies. PLoS One *10*, e0119467.

Bohorquez, D.V., Shahid, R.A., Erdmann, A., Kreger, A.M., Wang, Y., Calakos, N., Wang, F., and Liddle, R.A. (2015). Neuroepithelial circuit formed by innervation of sensory enteroendocrine cells. J. Clin. Invest. *125*, 782–786.

Bondurand, N., Natarajan, D., Thapar, N., Atkins, C., and Pachnis, V. (2003). Neuron and glia generating progenitors of the mammalian enteric nervous system isolated from foetal and postnatal gut cultures. Development *130*, 6387–6400.

Burns, A.J., and Douarin, N.M. (1998). The sacral neural crest contributes neurons and glia to the post-umbilical gut: spatiotemporal analysis of the development of the enteric nervous system. Development *125*, 4335–4347.

Burns, A.J., Goldstein, A.M., Newgreen, D.F., Stamp, L., Schafer, K.H., Metzger, M., Hotta, R., Young, H.M., Andrews, P.W., Thapar, N., et al. (2016). White paper on guidelines concerning enteric nervous system stem cell therapy for enteric neuropathies. Dev. Biol. *417*, 229–251.

Burns, A.J., Roberts, R.R., Bornstein, J.C., and Young, H.M. (2009). Development of the enteric nervous system and its role in

intestinal motility during fetal and early postnatal stages. Semin. Pediatr. Surg. *18*, 196–205.

Cooper, J.E., McCann, C.J., Natarajan, D., Choudhury, S., Boesmans, W., Delalande, J.M., Vanden Berghe, P., Burns, A.J., and Thapar, N. (2016). In vivo transplantation of enteric neural crest cells into mouse gut; engraftment, functional integration and long-term safety. PLoS One *11*, e0147989.

Costa, M., Brookes, S.J., and Hennig, G.W. (2000). Anatomy and physiology of the enteric nervous system. Gut *47* (*Suppl 4*), iv15–19, discussion iv26.

Fattahi, F., Steinbeck, J.A., Kriks, S., Tchieu, J., Zimmer, B., Kishinevsky, S., Zeltner, N., Mica, Y., El-Nachef, W., Zhao, H., et al. (2016). Deriving human ENS lineages for cell therapy and drug discovery in Hirschsprung disease. Nature *531*, 105–109.

Finkbeiner, S.R., Freeman, J.J., Wieck, M.M., El-Nachef, W., Altheim, C.H., Tsai, Y.H., Huang, S., Dyal, R., White, E.S., Grikscheit, T.C., et al. (2015). Generation of tissue-engineered small intestine using embryonic stem cell-derived human intestinal organoids. Biol. Open *4*, 1462–1472.

Friedt, M., and Welsch, S. (2013). An update on pediatric endoscopy. Eur. J. Med. Res. *18*, 24.

Furness, J.B. (2012). The enteric nervous system and neurogastroenterology. Nat. Rev. Gastroenterol. Hepatol. *9*, 286–294.

Furness, J.B., Callaghan, B.P., Rivera, L.R., and Cho, H.J. (2014). The enteric nervous system and gastrointestinal innervation: integrated local and central control. Adv. Exp. Med. Biol. *817*, 39–71.

Furness, J.B., Johnson, P.J., Pompolo, S., and Bornstein, J.C. (1995). Evidence that enteric motility reflexes can be initiated through entirely intrinsic mechanisms in the guinea-pig small intestine. Neurogastroenterol. Motil. *7*, 89–96.

Furness, J.B., Rivera, L.R., Cho, H.J., Bravo, D.M., and Callaghan, B. (2013). The gut as a sensory organ. Nat. Rev. Gastroenterol. Hepatol. *10*, 729–740.

Goldstein, A.M., and Nagy, N. (2008). A bird's eye view of enteric nervous system development: lessons from the avian embryo. Pediatr. Res. *64*, 326–333.

Grant, C.N., Mojica, S.G., Sala, F.G., Hill, J.R., Levin, D.E., Speer, A.L., Barthel, E.R., Shimada, H., Zachos, N.C., and Grikscheit, T.C. (2015). Human and mouse tissue-engineered small intestine both demonstrate digestive and absorptive function. Am. J. Physiol. Gastrointest. Liver Physiol. *308*, G664–G677.

Gremel, G., Wanders, A., Cedernaes, J., Fagerberg, L., Hallstrom, B., Edlund, K., Sjostedt, E., Uhlen, M., and Ponten, F. (2015). The human gastrointestinal tract-specific transcriptome and proteome as defined by RNA sequencing and antibody-based profiling. J. Gastroenterol. *50*, 46–57.

Grikscheit, T.C., Ochoa, E.R., Ramsanahie, A., Alsberg, E., Mooney, D., Whang, E.E., and Vacanti, J.P. (2003). Tissue-engineered large intestine resembles native colon with appropriate in vitro physiology and architecture. Ann. Surg. *238*, 35–41.

Hetz, S., Acikgoez, A., Voss, U., Nieber, K., Holland, H., Hegewald, C., Till, H., Metzger, R., and Metzger, M. (2014). In vivo transplantation of neurosphere-like bodies derived from the human postnatal and adult enteric nervous system: a pilot study. PLoS One *9*, e93605.

Hotta, R., Cheng, L.S., Graham, H.K., Pan, W., Nagy, N., Belkind-Gerson, J., and Goldstein, A.M. (2016). Isogenic enteric neural progenitor cells can replace missing neurons and glia in mice with Hirschsprung disease. Neurogastroenterol. Motil. *28*, 498–512.

Huang, M., Miller, M.L., McHenry, L.K., Zheng, T., Zhen, Q., Ilkhanizadeh, S., Conklin, B.R., Bronner, M.E., and Weiss, W.A. (2016). Generating trunk neural crest from human pluripotent stem cells. Sci. Rep. *6*, 19727.

Johann, V., Schiefer, J., Sass, C., Mey, J., Brook, G., Kruttgen, A., Schlangen, C., Bernreuther, C., Schachner, M., Dihne, M., et al. (2007). Time of transplantation and cell preparation determine neural stem cell survival in a mouse model of Huntington's disease. Exp. Brain Res. *177*, 458–470.

Kruger, G.M., Mosher, J.T., Bixby, S., Joseph, N., Iwashita, T., and Morrison, S.J. (2002). Neural crest stem cells persist in the adult gut but undergo changes in self-renewal, neuronal subtype potential, and factor responsiveness. Neuron *35*, 657–669.

Kunze, W.A., and Furness, J.B. (1999). The enteric nervous system and regulation of intestinal motility. Annu. Rev. Physiol. *61*, 117–142.

Lake, J.I., and Heuckeroth, R.O. (2013). Enteric nervous system development: migration, differentiation, and disease. Am. J. Physiol. Gastrointest. Liver Physiol. *305*, G1–G24.

Laughlin, D.M., Friedmacher, F., and Puri, P. (2012). Total colonic aganglionosis: a systematic review and meta-analysis of long-term clinical outcome. Pediatr. Surg. Int. *28*, 773–779.

Lee, H.T., Hennig, G.W., Fleming, N.W., Keef, K.D., Spencer, N.J., Ward, S.M., Sanders, K.M., and Smith, T.K. (2007). The mechanism and spread of pacemaker activity through myenteric interstitial cells of Cajal in human small intestine. Gastroenterology *132*, 1852–1865.

Lindley, R.M., Hawcutt, D.B., Connell, M.G., Almond, S.L., Vannucchi, M.G., Faussone-Pellegrini, M.S., Edgar, D.H., and Kenny, S.E. (2008). Human and mouse enteric nervous system neurosphere transplants regulate the function of aganglionic embryonic distal colon. Gastroenterology *135*, 205–216.e6.

Liu, L.W., Thuneberg, L., and Huizinga, J.D. (1994). Selective lesioning of interstitial cells of Cajal by methylene blue and light leads to loss of slow waves. Am. J. Physiol. *266*, G485–G496.

McCracken, K.W., Howell, J.C., Wells, J.M., and Spence, J.R. (2011). Generating human intestinal tissue from pluripotent stem cells in vitro. Nat. Protoc. *6*, 1920–1928.

Metzger, M., Bareiss, P.M., Danker, T., Wagner, S., Hennenlotter, J., Guenther, E., Obermayr, F., Stenzl, A., Koenigsrainer, A., Skutella, T., et al. (2009a). Expansion and differentiation of neural progenitors derived from the human adult enteric nervous system. Gastroenterology *137*, 2063–2073.e4.

Metzger, M., Caldwell, C., Barlow, A.J., Burns, A.J., and Thapar, N. (2009b). Enteric nervous system stem cells derived from human gut mucosa for the treatment of aganglionic gut disorders. Gastroenterology *136*, 2214–2225.e1-3.

Qu, Z.D., Thacker, M., Castelucci, P., Bagyanszki, M., Epstein, M.L., and Furness, J.B. (2008). Immunohistochemical analysis of neuron types in the mouse small intestine. Cell Tissue Res. *334*, 147–161.

Schneider, C.A., Rasband, W.S., and Eliceiri, K.W. (2012). NIH Image to ImageJ: 25 years of image analysis. Nat. Methods *9*, 671–675.

Spence, J.R., Mayhew, C.N., Rankin, S.A., Kuhar, M.F., Vallance, J.E., Tolle, K., Hoskins, E.E., Kalinichenko, V.V., Wells, S.I., Zorn, A.M., et al. (2011). Directed differentiation of human pluripotent stem cells into intestinal tissue in vitro. Nature *470*, 105–109.

Sulkowski, J.P., Cooper, J.N., Congeni, A., Pearson, E.G., Nwomeh, B.C., Doolin, E.J., Blakely, M.L., Minneci, P.C., and Deans, K.J. (2014). Single-stage versus multi-stage pull-through for Hirschsprung's disease: practice trends and outcomes in infants. J. Pediatr. Surg. *49*, 1619–1625.

Takahashi, T. (2003). Pathophysiological significance of neuronal nitric oxide synthase in the gastrointestinal tract. J. Gastroenterol. *38*, 421–430.

Timmermans, J.P., Barbiers, M., Scheuermann, D.W., Bogers, J.J., Adriaensen, D., Fekete, E., Mayer, B., Van Marck, E.A., and De Groodt-Lasseel, M.H. (1994). Nitric oxide synthase immunoreactivity in the enteric nervous system of the developing human digestive tract. Cell Tissue Res. *275*, 235–245.

Uesaka, T., Young, H.M., Pachnis, V., and Enomoto, H. (2016). Development of the intrinsic and extrinsic innervation of the gut. Dev. Biol. *417*, 158–167.

Watson, C.L., Mahe, M.M., Munera, J., Howell, J.C., Sundaram, N., Poling, H.M., Schweitzer, J.I., Vallance, J.E., Mayhew, C.N., Sun, Y., et al. (2014). An in vivo model of human small intestine using pluripotent stem cells. Nat. Med. *20*, 1310–1314.

Wieck, M.M., El-Nachef, W.N., Hou, X., Spurrier, R.G., Holoyda, K.A., Schall, K.A., Mojica, S.G., Collins, M.K., Trecartin, A., Cheng, Z., et al. (2016). Human and murine tissue-engineered colon exhibit diverse neuronal subtypes and can be populated by enteric nervous system progenitor cells when donor colon is aganglionic. Tissue Eng. Part A. *22*, 53–64.

Wilkinson, D.J., Bethell, G.S., Shukla, R., Kenny, S.E., and Edgar, D.H. (2015). Isolation of enteric nervous system progenitor cells from the aganglionic gut of patients with Hirschsprung's disease. PLoS One *10*, e0125724.

Workman, M.J., Mahe, M.M., Trisno, S., Poling, H.M., Watson, C.L., Sundaram, N., Chang, C.F., Schiesser, J., Aubert, P., Stanley, E.G., et al. (2017). Engineered human pluripotent-stem-cell-derived intestinal tissues with a functional enteric nervous system. Nat. Med. *23*, 49–59.

Zhou, S., Szczesna, K., Ochalek, A., Kobolak, J., Varga, E., Nemes, C., Chandrasekaran, A., Rasmussen, M., Cirera, S., Hyttel, P., et al. (2016). Neurosphere based differentiation of human iPSC improves astrocyte differentiation. Stem Cells Int. *2016*, 4937689.